1 *Article*

2 3 4 Assessing the Impact of Man–Made Ponds on Soil Erosion and Sediment Transport in Limnological Basins

5 Mario J. Al Sayah [1,2,3], Rachid Nedjai [2], Konstantinos Kaffas [4], Chadi Abdallah [1,*] and Michel Khouri [2]

6 7   [1]   National Council for Scientific Research – Remote Sensing Center, Beirut – Lebanon; chadi@cnrs.edu.lb; mario.alsayah@gmail.com

8 9   [2]   Centre de Recherches en Sciences et Ingénierie – Lebanese University Faculty of Engineering II, Roumieh – Lebanon; mkhuri@ul.edu.lb; mario.alsayah@gmail.com

10 11   [3]   Centre d'Études et de Développement des Territoires et de l'Environnement – Université d'Orléans – Orléans, France ; rachid.nedjai@univ-orleans.fr; mario.al-sayah@etu.univ-orleans.fr

12 13   [4]   Faculty of Science and Technology, Free University of Bozen–Bolzano, 39100 Bozen–Bolzano, Italy; Konstantinos.Kaffas@unibz.it; kostaskaffas@gmail.com

14   *   Correspondence: chadi@cnrs.edu.lb; Tel.: (+961 00961 3 534 436; Tell: 00961 1 840 260/1/2/3/4; Fax: 00961 1)

15

16 17 18 19 20 21 22 23 24 25 26 27 28 29 **Abstract:** The impact of ponds on basins has recently started to receive its well–deserved scientific attention. In this study, pond–induced impacts on soil erosion and sediment transport were investigated at the scale of the French Claise basin. In order to determine erosion and sediment transport patterns under current conditions, the CORINE erosion and SWAT models were used. The impact of ponds on the studied processes was revealed by means of land cover change scenarios, using ponded versus pondless inputs. Results show that under current conditions (pond presence), 12.48% of the basin corresponds to no–erosion risk zones (attributed to the dense pond network), while 65.66% corresponds to low–erosion risk, 21.68% to moderate–erosion risk and only 0.18% to high–erosion risk zones. The SWAT model revealed that ponded sub–basins correspond to low sediment yields areas, in contrast to the pondless sub–basins, which yield appreciably higher erosion rates. Under the alternative scenario, erosion risks shifted to 1.12%, 0.52%, 76.8% and 21.56% for no, low, moderate and high–erosion risks, respectively, while the sediment transport pattern of the Claise completely shifted to higher sediment yield zones. This approach solidifies ponds as powerful man–induced modifications to hydro/sedimentary processes.

30 31 32 **Keywords:** soil erosion, sediment transport, SWAT, CORINE erosion model, ponds, Brenne, limnology, land cover change

33 1. Introduction

34 35 36 37 38 39 40 41 42 43 44 45   Understanding the impact of land occupation (land use/cover) on basin processes, such as rainfall–runoff and soil erosion, is an integral part of land and water management–oriented decisions [1,2]. The processes of soil erosion and sediment transport take part in van Rijn's (1993) [3] sedimentary cycle, and often are the main causes of soil loss in basins [4]. Although these processes are of natural origin [5], the interaction between climate, soil, topography, land use, and land cover significantly influence erosion rates and sediment loads [6,7]. Soil loss due to these processes is a frequent problem that hydrologists, land planners and basin managers will need to deal with [8]. Accordingly, soil erosion quantification in erosion–prone areas, with the highest accuracy possible, provides a complete knowledge of soil loss hotspots and allows prioritized treatment measures for supporting land processes in the concerned basin [9]. Subsequently, the reliable assessment and representation of sediment yields – which depend on the cascading effect of soil erosion – allows an in–depth understanding of the soil erosion–sediment link at the basin scale [9].

46   For representing both processes, several models have been developed and used extensively to
47   replace the conventional assessment methods, i.e. the Water Erosion Prediction Project (WEPP)
48   [10,11], the Universal Soil Loss Equation (USLE) [12], the Modified Universal Soil Loss Equation
49   (MUSLE) [13], the Revised Universal Soil Loss Equation (RUSLE) [14,15] and the Soil and Water
50   Assessment Tool (SWAT) [16]. SWAT is one of the most widely used basin models. It has been
51   applied extensively in modeling the impact of land occupation changes, under different scenarios
52   and different contexts [17,19]. The widespread use of SWAT can be justified by its sensitivity and
53   flexibility towards the land occupation input [20], its adaptability to different contexts – even to those
54   with data scarcity [21] –, its simple data requirements and ease of computation [22], as well as the
55   straightforward calibration through its stand–alone SWATCUP interface [23].

56   Despite abundant research regarding the impact of land occupation on soil loss, few studies
57   focus on the particular case of small water bodies and their effect as a land occupation class [24].
58   Small water bodies like ponds and wetlands are considered as the most amplified form of man–
59   induced modifications to the hydro–sedimentological system of basins [25]. Ponds represent a total
60   of over 90% of global standing water bodies, 30% of global standing waters by surface area [26] and
61   form the most widespread aquatic habitat dominating the continental standing waters in Europe [27].
62   Despite their well–documented significance [28], abundant numbers and increasing proliferation
63   [29], ponds have not received considerable scientific attention compared to rivers and lakes [27]. It is
64   worth mentioning that research regarding ponds in Europe has tripled in the last decade [30], where
65   results showed that ponds contribute significantly to several basin related processes [31]. Examples
66   of these processes are sediment interception [32], removal of pollutants for river protection [33],
67   nutrient recycling [34], regulation of hydrological flows [35], biogeochemistry [31] and climate [36].
68   In addition to their environmental role, ponds have a well–known value for housing and sustaining
69   biodiversity, supporting livelihoods, local economies, and taking part in the socio–cultural heritage
70   of the settings they are located in [37].

71   Under the hydro–sedimentological scope, particularly, ponds have shown to retain as much as
72   90% of sediments transported in basins [38]. Consequently, ponds have been heavily blamed for
73   rupturing the ecological and sedimentary continuum of the basins they belong to [39]. The disruptive
74   effect of ponds is due to the increase of residence time of waters, resulting in a decline in the temporal
75   variation of the main discharge [40]. Accordingly, the deceleration of overland flow allows
76   suspended particles to settle under the effect of their weight, causing a reduction in the amount of
77   sediments entrained by water, making ponds sediment sinks [40]. However, this effect strongly
78   depends on their position in the basin, their depth, volume, slope [41], as well as the surrounding
79   land occupation [42]. Winfield Fairchild and Velinsky (2006) [43], showed that ponds located
80   upstream of rivers – considering their sediment retention capacity – are capable of creating a state of
81   imbalance in the geochemical and hydro–sedimentary status of the underlying rivers. Consequently,
82   the Directive Cadre sur l'Eau (DCE) [44] stresses the need to assess the impact of hydromorphological
83   elements that are capable of influencing hydrologic pathways, river morphology, width, and
84   continuity.

85   Beyond the contribution of isolated ponds, connected networks of ponds were found to
86   contribute to basin processes at higher rates than lakes or even rivers [45,46]. Particularly in France,
87   ponds are mainly concentrated in three regions: the Sologne region, Brenne (Central France) and
88   Dombes (Eastern France). In response to DCE recommendations, this study aims to assess the impact
89   of man–made ponds on soil erosion and sediment transport, at the scale of the Indre portion of the
90   Claise basin. This part corresponds to the Brenne Natural Regional Park that houses 4500 waterbodies
91   (ponds, marshes, and small water surfaces) 2179 of which are located in Claise, being part of an
92   interconnected network. To evaluate erosion risks in the Claise, the CORINE (1992) Erosion Risk
93   model will be used, since it presents a simplification of the reliable USLE model [1] and given that
94   no–erosion field data, for the Claise, were available for the study. SWAT is employed to assess the
95   impact of ponds on the Claise's hydro–sedimentary regime. This choice is owed to SWAT's ability to
96   simulate the physical processes that occur in ponds, which in turn allows an accurate representation
97   of pond containing basins [38]. This is achieved through the SWAT Pond (.pnd) input file that makes

98   SWAT one of the few hydrological models having an input for ponds [47]. Related studies have
99   assessed the behavior of ponds using SWAT [38,75] and highlighted the efficiency of SWAT on this
100   part.
101   The impact of the Claise's ponds on erosion and sediment transport will be assessed by testing
102   alternative scenarios, where the land occupation input for both models will be simulated with and
103   without ponds. By this approach, a quantification of the pond impact can be obtained. The presented
104   work serves as a decision–oriented tool for basins similar to the Claise, where pond proliferation has
105   been halted until a proper understanding of their effect is established. In addition, analysis of soil
106   erosion risks and sediment transport is useful for conservation measures that aim towards
107   prolonging the useful life of these small water bodies or for ceasing their proliferation.

108   **2. Materials and Methods**

109   *2.1. Study area*

110   The Brenne portion of Claise basin (Figure 1) covers an area of 707 km^2 and is one of the three
111   entities housing the 4500 ponds of the Brenne Natural Regional Park, that are mostly grouped in the
112   form of interconnected chains [36]. Within the Claise, 2179 of the Brenne waterbodies, along with the
113   Five Bonds channel (Blizon), are the main contributors [48] to the 87.6 km long and with an average
114   discharge of 4.5 m^3/s Claise River [49]. The basin is mostly dominated by a degraded oceanic climate
115   with a mean temperature of 11°C and average annual precipitation of 700 mm [50]. As to its
116   topographical profile, the basin is considered to be a flat plain, with 99% of its surface falling into the
117   0–5% slope class, while its altitude varies between 76 m and 181 m. The six poorly–permeable soil
118   classes of the basin, are mostly dominated by Luvisols [36,51]. At a combined state, the Claise's
119   challenging pedology, flat topographical setting and quasi–impermeable lithology, have resulted in
120   the stagnation of incoming water leading to the formation of natural ponds [52]. According to
121   Bennarous (2009) [37], however, these ponds are not only a product of natural processes but also an
122   anthropogenic adaptation to a poorly drained domain and a source of economic livelihood
123   (aquaculture) in an environment of limited productivity. As a result of intensive pond proliferation
124   throughout time, the basin has acquired a particular hydrographic network characterized by an
125   abundance of different kinds of water bodies. Despite its richness, nonetheless, the hydrographic
126   network of the basin is randomly organized and presents severe fragmentation [53]. In contrast to the
127   evolving pond proliferation, the land occupation setting of the Claise has been relatively unchanged
128   for the last nineteen years, mainly displaying a dominance of an interlocked mosaic of forests,
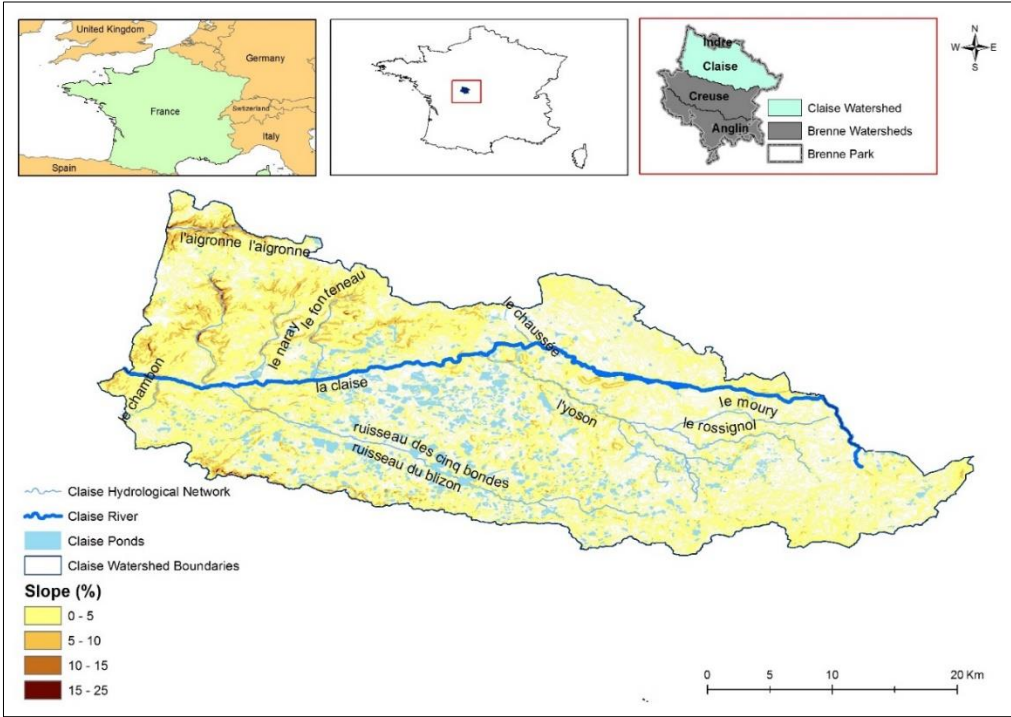129   grasslands and agricultural areas [53].

131   **Figure 1.** Study area

132   *2.2. The SWAT Model: Basins and Impoundments*

133   SWAT is one of the few hydrological models that have an input for ponds [47], which makes it
134   an ideal tool for this study. SWAT is a semi–physical deterministic distributed and continuous
135   hydrologic model that functions at a daily time step with options for sub–hourly routing, as well [59].
136   It is a quite complex model with significant input data demands. However, the basic components can
137   be readily obtained and are relatively simple [18]. Essential inputs consist of weather data, Digital
138   Elevation Model (DEM), soil, and land occupation maps [55]. Based on these inputs, SWAT divides
139   the basin into sub–basins, which further divides into smaller Hydrological Response Units (HRUs)
140   [56]. HRUs are defined as units with homogeneous land occupation, topography and pedological
141   properties [57]. These are generated in order to lump somewhat similar areas scattered through the
142   basin into a single unit, simplifying the model's run by avoiding unpractical simulations while
143   accounting for the diversity of different factors in the basin [58]. Within SWAT, ponds are defined as
144   waterbodies, being an integral part of a sub–basin's hydrological network; they are capable of
145   intercepting surface runoff [59], thereby modifying the hydro–sedimentary behavior of the basin.
146   Since this work targets the erosion/sedimentary behavior of the SWAT model, only their related
147   equations will be presented. Further details can be found in Neitsch et al. (2011) [47].
148   Soil erosion is calculated based on the Modified Universal Soil Loss Equation (MUSLE) using
149   the following formula [59]:

$$SY = 11.8 \cdot (Q \cdot q \cdot A) \cdot 0.56 \cdot K \cdot C \cdot P \cdot LS \cdot F \tag{1}$$

150   where: *SY* is the HRU sediment yield (metric tons); *Q* is the surface runoff volume (mm water); *q* is
151   the peak runoff rate (m^3/s); *A* is the area of the HRU (ha); *K* is the Universal Soil Loss Equation (USLE)
152   soil erodibility factor; *C* is the USLE cover and management factor; *P* is the USLE support practice
153   factor; *LS* is the USLE topographic factor; and *F* is the coarse fragment factor.
154   It should be noted that MUSLE virtually calculates the sediment yields due to soil erosion that
155   reaches the main streams of the sub–basins in a unit of time. This is the reason why sediment delivery
156   ratios are not required, contrarily to USLE and RUSLE [60].
157   The mass balance equation of sediment in ponds is described by the following formula [47]:

$$sed_{wb} = sed_{wb,i} + sed_{flowin} - sed_{stl} - sed_{flowout} \qquad (2)$$

where: sed_{wb} is the amount of sediment at the end of the day; $sed_{wb,i}$ is the amount of sediment at the day's beginning; sed_{flowin} is the amount of sediment provided from inflows; sed_{stl} is the amount of settled sediments; and $sed_{flowout}$ is the amount of sediment transported as outflow. All components are expressed in metric tons.

2.3. The CORINE Erosion Model

The CORINE erosion model is a simplification of the USLE model. In the CORINE model, erosion risks are classified on a scale of 0 to 3, with 0 corresponding to the no–erosion class, 1 to low erosion risks, 2 to moderate erosion risks and 3 to high–erosion risks [61]. For the estimation of erosion using the CORINE model, parameters such as soil erodibility, climate erosivity, topography (slope) and LU/LC (vegetation cover) are required [61]. Each parameter, in turn, consists of several sub–factors, and is classified according to the CORINE model into respective indices (Figure 2). Once established, the soil erodibility index is combined with climate erosivity and slope, to yield the Potential Soil Erosion risk map. Subsequently, the Potential Soil Erosion risk map indices (0 to 3) are crossed with those of the vegetation cover to yield the Actual Soil Erosion map.
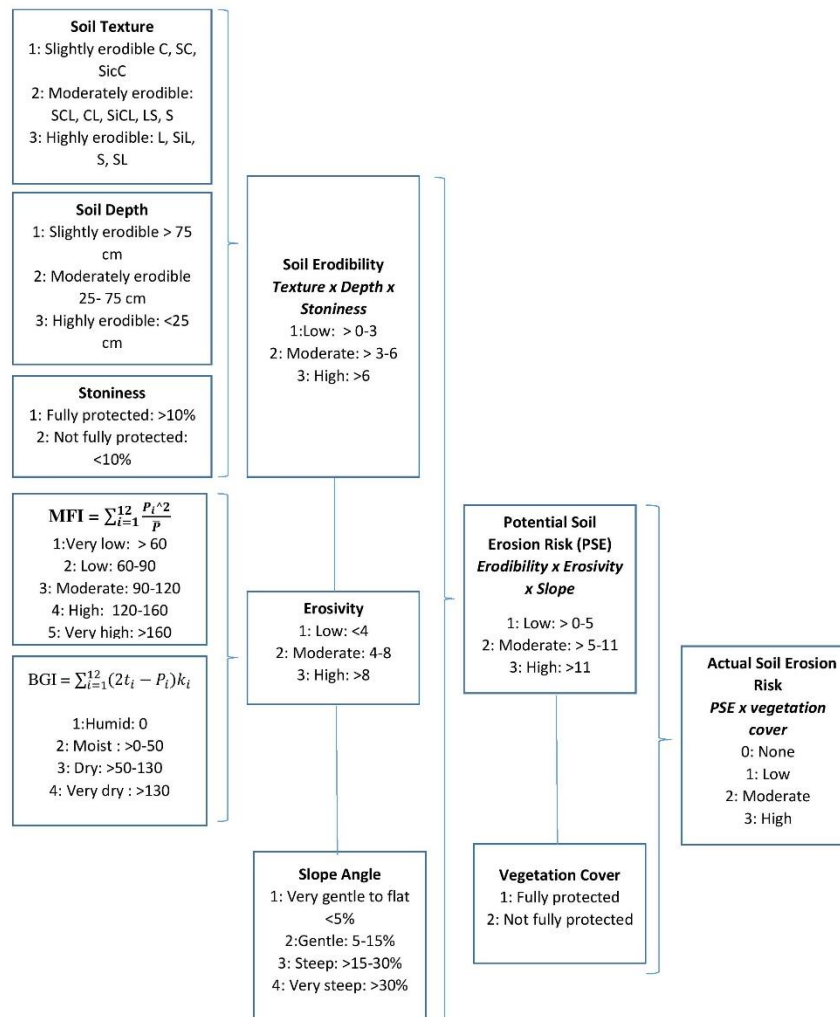

Figure 2. CORINE model framework, MFI: Modified Fournier Index [62] Pi is the total precipitation in month i and P̄ is the mean annual total precipitation. BGI: Bagnouls–Gaussen Index [63] ti the mean temperature for the month i, Pi the total precipitation in month i and ki the proportion of the month in which 2ti – Pi > 0. Source [61]

176   *2.4. Input data and adaptation to the SWAT and CORINE models*

177   The input data used in this study, along with a short description, are summarized in Table 1.

178

179   **Table 1.** CORINE erosion model and SWAT input data

Input Data	Source	Date	Description
Topography – DEM	Institut Géographique National (IGN) – France	2010	25 m resolution
Soil map	Harmonized World Soil Database (HWSD) [51]	2008	30 arc–second raster database
Weather data	Weatherlink Pro 2 weather stations, source : R. Nedjai	2016–2018	Daily time step
	Système d'Analyse Fournissant des Renseignements Adaptés à la Nivologie (SAFRAN) model (Durand et al., 1993)	1970–2018	
Land Use Land Cover map	Digitized from aerial photography and cross–checked against ancillary maps	2018	Ortho–rectified aerial photography – Resolution: 0.5 m verified against ancillary maps: CORINE 2012 land use land cover maps

180

181   ArcSWAT version 2012.10_3.19 was applied in an ArcGIS 10.3 environment to perform
182   simulations at a daily time step for the period 1970–2018. The first seven years of the simulation, from
183   1970 to 1976, were used for the model's warm up. The calibration and validation phases of the model
184   were carried out by means of comparison between simulated discharges and measured discharge
185   data from the station L6202040 – La Claise au Grand–Pressigny [Pont de Fer], obtained from
186   EauFrance Banque HYDRO – Ministère de l'Ecologie, de l'Energie, du Développement Durable et de
187   l'Aménagement du Territoire (MEEDDAT)/Direction Générale de la Prévention des Risques (DGPR)/
188   Service des Risques Naturels et Hydrauliques (SRNH). Due to the unavailability of sediment records
189   for this study, only a hydrologic calibration was performed. However, surface runoff and stream flow
190   – regardless the approach used to model the sedimentary cycle – are the driving forces of runoff and
191   streambed erosion, as well as of overland and stream sediment transport [59]. Hence, one might say
192   that the calibration of the sediment part of the study might be implicit, but nonetheless robust.
193   According to Hallouz et al. (2018) [66], a calibrated hydrologic model gives a certain degree of
194   reliability to the sedimentary output.

2.4.1. DEM: Topographic effect and use in both models

In the CORINE model, DEM is used to extract the topographic parameter by means of slope computation. The slope angles of the study area were obtained using the "slope" tool of ArcGIS. Subsequently, the slope raster was classified, with respect to the CORINE's model indices, into (1) very gentle to flat (<5%), (2) gentle (5–15%), (3) steep (15–30%), and (4) very steep (>30%).

In SWAT, the DEM is used for the extraction of the topographic parameters and for representing the basin's physical parameters such as slopes, flow direction and accumulation, delineation of the hydrologic network, and basin partitioning [67]. After inputting the DEM into SWAT, the basin was initially divided into 25 sub–basins using SWAT's watershed delineator. However, given the presence of a great number of waterbodies, and their impact on output accuracy, the number of sub–basins was increased to 35. The purpose of increasing sub–basins' number was to increase the spatial resolution for more detailed representation of the basins' processes [68]. Since the SWAT model allows only one pond per sub–basin [38] during sub–basins' delineation, the largest number of ponds was included in each in order to ensure maximal representation of pond–induced processes. Further, all ponds within each sub–basin were lumped and the outlets of the sub–basins were chosen to coincide with those of the ponds in order to maximize their representation and account for their effect. The SWAT delineated hydrologic network was in turn verified against a pre–defined stream network in order to ensure and improve its accuracy.

2.4.2. Pedology: Adaptation to the different requirements of the models used

The pedological composition of the Claise was determined from the Harmonized World Soil Database (HWSD) [51]. For the CORINE model, soil texture was determined using the USDA textural triangle after inputting the respective percentages of sand, silt and clay for each soil group obtained from the HWSD. Texture was then classified with respect to CORINE indices. The parameters of depth and stoniness were treated and classified similarly. After obtaining the texture, depth and stoniness sub–factors, the three layers were input into the "raster calculator" in analogy to Figure 2.

For the SWAT model, the hydrologic soil group of each class was assigned following the United States Department of Agriculture [69] Soil Conservation Service (SCS) soil survey. Bulk densities were computed using the Soil Water Characteristics software following Saxton and Rawl (2006) [70] equations that were shown to have adequate accuracy for bulk density computation by Al Sayah et al. (2019) [71]. Likewise, the available water capacity and saturated hydraulic conductivities were also computed using the same software. Organic Carbon content was determined by multiplying the organic matter content derived from the HWSD by 0.58, since organic carbon forms around 58% of the soil's organic matter as a rule of thumb [72]. Sand, silt, and clay percentages, as well as the rock fragment contents were extracted from the HWSD. The USLE_K factor was computed following the formula presented in the SWAT documentation [59], while soil surface albedo was determined using the following formula [73]:

$$Soil\ albedo\ (0.3–2.8\ \mu m) = 0.069 \cdot (color\ value) – 0.114 \tag{3}$$

After building the soil database, all parameters were reclassified in SWAT using user–adapted look–up tables for integration into the SWAT database.

2.4.3. Weather data: Forcing on–field weather data to a meteorological model

Weather data was obtained from two sources, on–field weather station data and Météo France's Système d'Analyse Fournissant des Renseignements Adaptés à la Nivologie (SAFRAN) model [64]. The SAFRAN model was used since it contains records for the period 1970–2018 while the weather stations, located next to a pond network were used to account for the climatic regulating effect reported by Nedjai et al. (2018) [36]. SAFRAN was used in order to provide a large time span for the study. Moreover, the SAFRAN was validated by test–correlation with weather station data using Pearson's correlation coefficient "r" [74]. Prior to correlation, harmonization of both datasets was

241 performed since the weather stations record parameters at the hourly time step, while SAFRAN
242 simulates at the daily time step. Results of the correlation are presented in Table 2.

243   **Table 2.** Validation testing of the SAFRAN model against measured on field–data for revealing SAFRAN's
244   validity for use.

245

Weather Stations parameters	SAFRAN parameters	Parameter label	Correlation, r
Temp Out	T_Q	Average temperature (˚C)	0.98
Hi Temp	TSUP_H_Q	Maximal temperature (˚C)	0.98
Low Temp	TINF_H_Q	Minimal temperature (˚C)	0.97
Out Hum	HU_Q	Relative humidity (%)	0.97
Wind Speed	FF_Q	Wind speed (m/s)	0.83
Rain	PE_Q	Efficient rainfall (mm)	0.64
Solar Rad.	SSI_Q	Incoming solar radiation (J/cm^2)	0.98

246
247 For the CORINE model, the rainfall and temperature parameters are used for computation of the MFI
248 and BGI indices following their respective formulas (Figure 2); these indices were then used to
249 calculate erosivity following the workflow of Figure 2. In SWAT, the weather database was built
250 using the WGN maker macro tool [75] and input into the SWAT database.

251 2.4.4. Land use and land cover: A particularly rich natural limnological setting

252   The land occupation map of the Claise was obtained by on–screen digitizing of aerial
253 photography at 0.5 m resolution. Such fine scale was used in order to ensure a detailed representation
254 of the study area, particularly to account as accurately as possible for the scale of ponds.
255   For the CORINE model, the obtained land occupation map was reclassified into fully protected
256 (forest, permanent pasture and scrublands) and not–fully protected (cultivated or bare land) areas as
257 demonstrated in Table 3.
258
259   **Table 3**. Numerical distribution of the land occupation setting of the Claise basin

Land occupation class	Area (km²)	Percentage (%)	CORINE vegetation cover index
Clear broad–leaved forest	2.21	0.31	1

Clear mixed forest	0.90	0.13	1
Coniferous forest	26.94	3.81	1
Dense broad–leaved forest	163.58	23.11	1
Dense mixed forest	27.00	3.82	1
Field crops in medium to large terraces	19.14	2.70	2
Fruit trees	0.20	0.03	2
Grassland	207.04	29.26	1
Inland marshes	4.01	0.57	1
Low density urban tissue	3.24	0.46	2
Medium density urban tissue	1.76	0.25	2
Mineral extraction site	0.09	0.01	2
Non–irrigated field crops	151.17	21.36	2
Pond	79.47	11.23	0
River	0.55	0.08	0
Scrubland	2.80	0.40	1
Scrubland with some bigger dispersed trees	15.36	2.17	1
Urban expansion site	0.01	0	2
Urban sprawl on clear wooded lands	0.01	0	2
Urban sprawl on field crops	1.01	0.14	2
Urban sprawl on grassland	1.20	0.17	2

In the case of SWAT, land use and land cover classes were reclassified into SWAT's classes. Particular attention was given to the water (in SWAT terms WATR) classes. As reported by Jalowska and Yuan (2019) [38], the reason for this is that though SWAT allows the creation of HRUs with WATR, water bodies should be modeled either as reservoirs or ponds. [76,38] have shown that an accurate representation of basin processes requires the integration of the SWAT model's impoundments function. Furthermore, Jalowska and Yuan (2019) [38] highlighted the importance of considering impoundments such as ponds by testing scenarios of impoundment integration versus impoundment disregarding in a basin covered by only by 3% of impoundments. Results confirm that simulations were considerably affected even with this small cover. In the same manner, Jalowska and Yuan (2019) [38] simulated different scenarios following integration or absence of impoundments like reservoirs rather than just a normal "water" land occupation class. They noted that disregarding impoundments leads to a series of uncertainties starting by an inaccurate SWAT performance, which in turn leads to inefficient calibration efforts, and overall inaccurate model performance.

After computing the slope, erosivity and soil erodibility indices, the Potential Soil Erosion risk map was constructed. By combining the Potential Erosion risk map to the vegetation cover layer in the "raster calculator" tool and crossing each ones indices, the Actual Soil Erosion risk Map was obtained.

3. Results

3.1. CORINE erosion model outputs for the Claise basin

In the following sections, the erosion assessment for the Claise is presented and each component is detailed accordingly.

3.1.1. Soil erodibility

Soil erodibility is presented in Figure 3. The dominant textural class in the basin was found to be loam (68.4%) followed by loamy sand (28.75%), while the remainder percentages are clay (2.48%) and sand (0.34%). In terms of texture, since most of the study area is covered by loam with respect to [61], the study area predominantly falls into the highly erodible class. In terms of soil depth, 94.6% of the Claise fits to the slightly erodible class (1000 mm > 750 mm), while the remainder 5.4% rests within the moderately erodible class (300 mm, corresponding to the 250–750 mm class). As far as stoniness is concerned, only 6% of the Claise is under the fully protected cover.
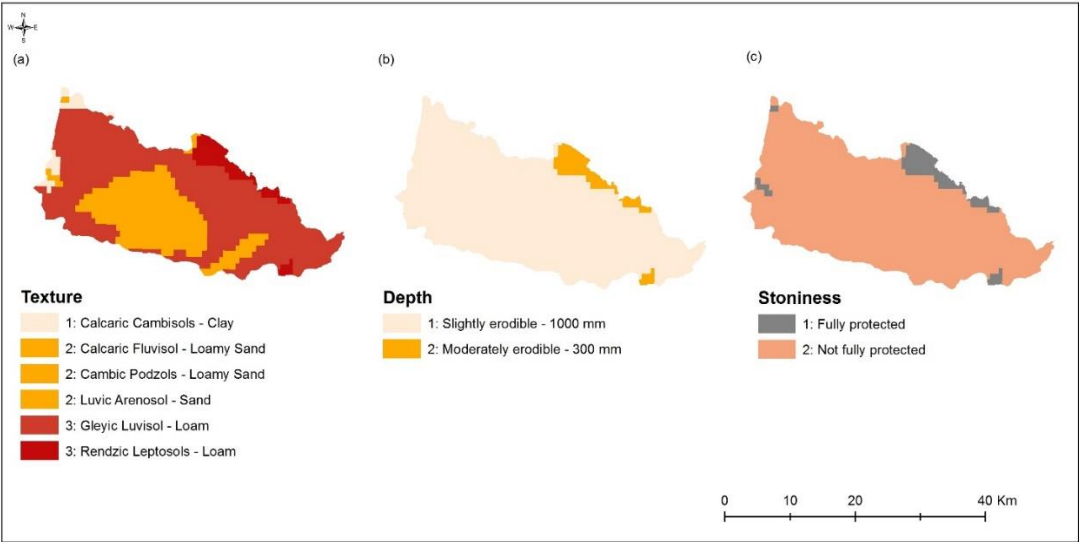

Figure 3. Spatial distribution of soil erodibility parameters (a) texture; (b) depth; and (c) stoniness and class descriptions of the Claise with their respective indices.

Table 4 provides the numerical description of the soil's erodibility components.

Table 4. Numerical distribution of soil erodibility parameters and corresponding covered areas

Parameter	CORINE Class	Area (km²)	Percentage (%)
Soil texture	1: Slightly erodible (clay)	17.53	2.48
	2: Moderately erodible (Loamy sand and sand)	205.88	29.12 (28.77 and 0.35)
	3: Highly erodible (Loam)	483.59	68.4
	Total	**707**	**100**
Soil depth	1: Slightly erodible (>1000 mm)	668.82	94.6
	2: Moderately erodible (250–750 mm)	38.18	5.4
	Total	**707**	**100**

	1: Fully protected (>10%)	43.26	6.12
Stoniness	2: Not fully protected (<10%)	663.73	93.88
	Total	**707**	**100**

298
299   By inputting the texture, depth and stoniness parameters into the "raster calculator" tool of
300 ArcGIS, the soil erodibility raster was generated and then reclassified using the "reclassify" tool
301 (Figure 4).
302

Soil Erodibility Risks of the Claise
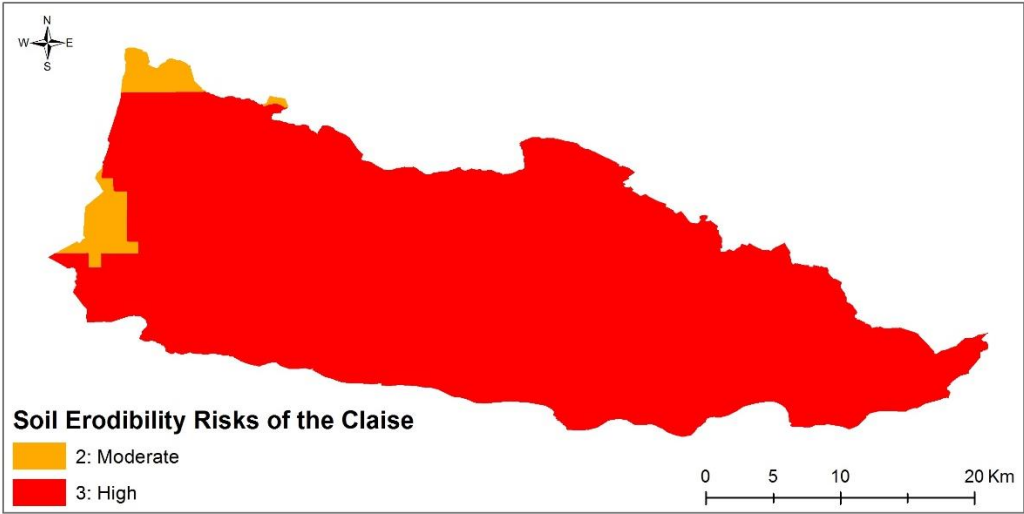- 2: Moderate
- 3: High

303
304 **Figure 4.** Soil erodibility map of the Claise classified according to the CORINE indices.
305

306   As seen in Figure 4, the generated soil erodibility map revealed that about 96.83% (684.37 km²)
307 of the study area is covered by highly erodible soils while the remainder 3.17% (22.63 km²)
308 correspond to moderate–risk areas. This fact is mainly due to the textural distribution of soil and the
309 little stone cover of the Claise basin.

310 3.1.2. Erosivity in a degraded oceanic climate setting

311   Meteorological data of the study area is presented in Table 5. As seen, no dry month exists in the
312 Claise and highest temperatures are recorded during the month of July making the basin subject to
313 continuous precipitation.
314
315   **Table 5.** Average temperature and precipitations for the Claise basin (1970–2018)

Month	Jan	Feb	Mar	Apr	May	Jun	Jul	Aug	Sep	Oct	Nov	Dec
Average temp. (˚C)	4.7	5.2	7.8	10.4	14.3	17.9	20.1	19.7	16.1	11.8	7.7	4.8
Precipitation (mm)	416	677	1106	1526	1782	2045	2108	1826	1356	818	482	361

316
317   MFI was found to be 80, corresponding to the low variability class. This signifies evenly
318 distributed rainfall, thus reducing risks of climate–induced soil erosion [78]. The Bagnouls–Gaussen
319 aridity Index (BGI) on the other hand, was found to be "0", signifying that the study area corresponds
320 to the humid regime as a result of its oceanic influence. In terms of CORINE erosivity, the Modified
321 Fournier Index (MFI) belongs to class 2 variability (low), while BGI corresponds to class 1 (humid).

322 Accordingly, the erosivity index of the Claise watershed was found to be 2, corresponding to the low
323 erosivity class.

3.1.3. Topography (slope): A reduced effect in a flat setting

325 Using the "slope" tool in ArcGIS, slope angles were extracted from the DEM. Figure 5 displays
326 the slope of the Claise basin and the adapted reclassified raster following CORINE classification.
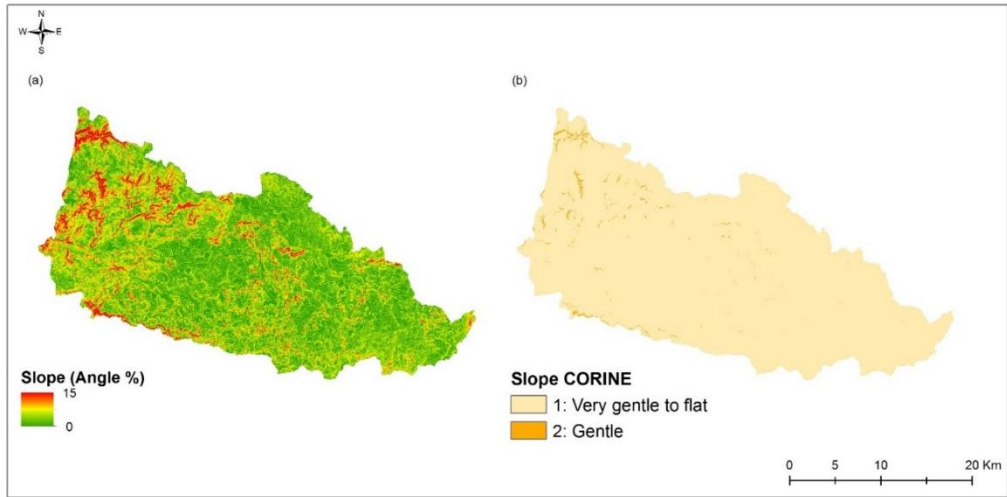327

328
329 **Figure 5.** (a) Slope angle of the Claise and (b) corresponding CORINE indices description.
330

331 From Figure 5, it can be observed that the Claise presents a dominantly flat topography with a
332 maximum slope of 15°. In CORINE terms, 99.3% (702.051 km²) of the study area corresponds to "very
333 gentle to flat" slope class (< 5°) and 0.7% (4.94 km²) to the "gentle" slope category (5°–15°). The
334 particular setting of low relief and small slope significantly plays a role in the reduction of erosion
335 generated by runoff [81], despite the high soil erodibility risks.

3.1.4. Potential Soil Erosion Map

337 By overlaying soil erodibility, topography and erosivity, using the "raster calculator" tool, the
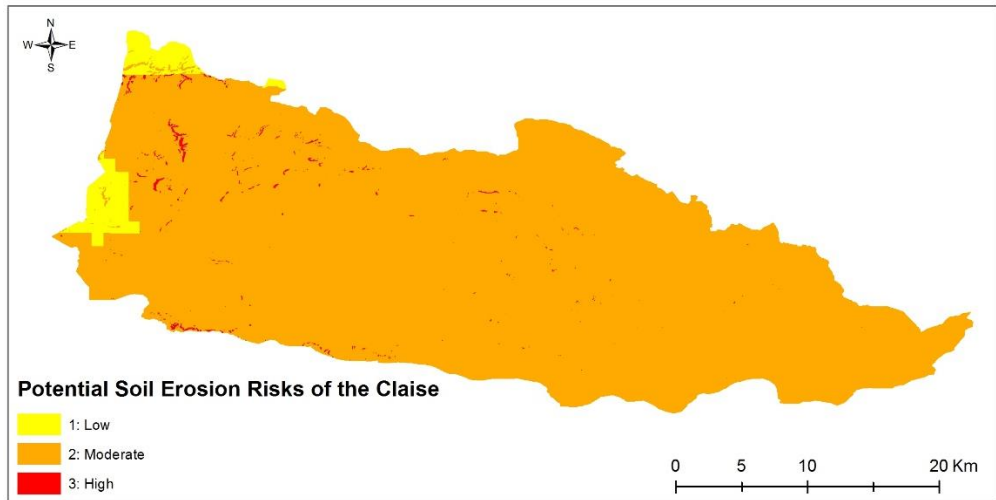338 Potential Soil Erosion risk map was obtained (Figure 6) following the formula presented in Figure 2.
339

340
341 **Figure 6.** Potential Soil Erosion (PSE) risk map of the Claise basin.
342

343 From Figure 6, low–erosion risks present 3% (21.22 km²), moderate risks present 96.5% (682.25
344 km²) and high risks form 0.5% (3.53 km²). These percentages, however, reflect only the potential risks

345   without considering the vegetative cover. The slope effect and equal repartition of precipitation, as
346   reflected by the MFI values and the absence of arid periods (low BGI), are potentially responsible for
347   moderating the soil erodibility map yielding the dominantly moderate Potential Soil Erosion risks.

348   3.1.5. Vegetation cover: The presence/absence effect of ponds

349   This factor is the focal point of this study since by slightly changing this parameter the outcome
350   changes significantly. At this point, two vegetative cover scenarios are presented: the first presents
351   the actual setting of the Claise accounting for the presence of ponds, while the second simulates a
352   scenario where ponds are removed to assess the difference in erosion outcomes with and without
353   their presence. This last step allowed to quantify the impact of ponds on erosion in the Claise basin.
354   In the second scenario, the land occupation group "ponds" was changed to their surrounding class
355   (grasslands).
356   The large area of ponds, which makes up around 11% of the Claise (Table 3), displays their
357   potential role as modifiers basin processes. Figure 7 presents the two considered vegetation covers as
358   inputs for crossing with the Potential Soil Erosion risk map to yield two different Actual Soil Erosion
359   risk maps. These maps were then compared to evaluate the effect of the presence and absence of
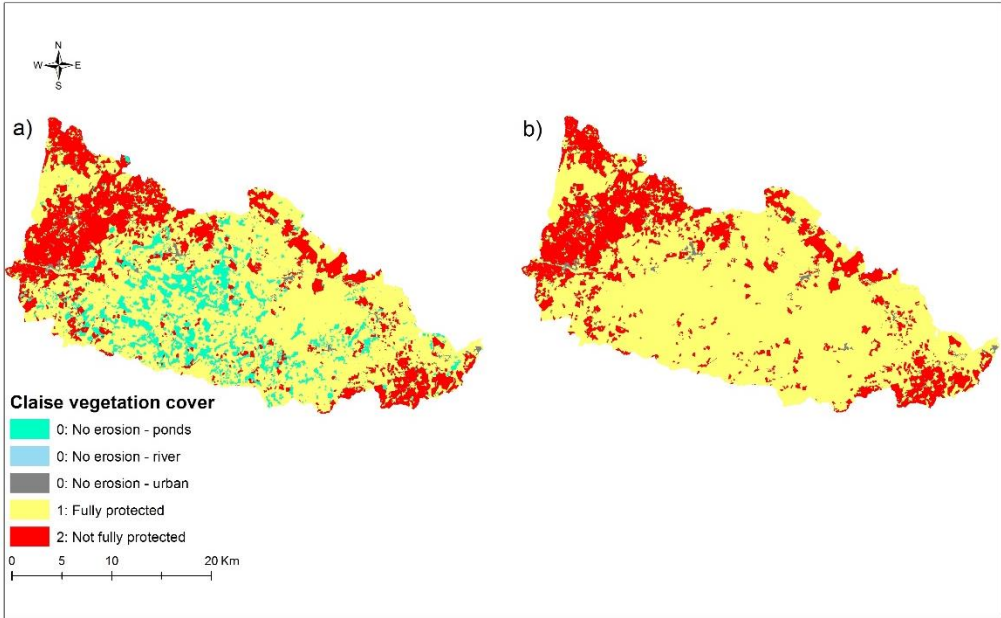360   ponds and their role on erosion.
361

362
363   **Figure 7.** (a) Current Claise vegetation cover and (b) Alternative vegetation cover and corresponding CORINE
364   classification; 1: fully protected, 2: not fully protected.
365

366   Class 0 refers to land cover categories that are not considered in CORINE; these categories are
367   urban areas and water bodies, while classes 1 and 2 refer to the fully protected and not fully protected
368   covers. From Figure 6(b), 72.5% of the Claise basin corresponds to the fully protected class, while
369   27.5% of the study area is occupied by not fully protected cover. To assess the impact of pond
370   presence, the second scenario of replacing ponds by their surrounding cover was performed.

371   3.1.6. Actual Soil Erosion maps under current and alternative scenarios

372   The two Actual Soil Erosion risks maps were produced by multiplying the respective indices of
373   the Potential Soil Erosion risk map and the two vegetation cover scenarios using the "raster
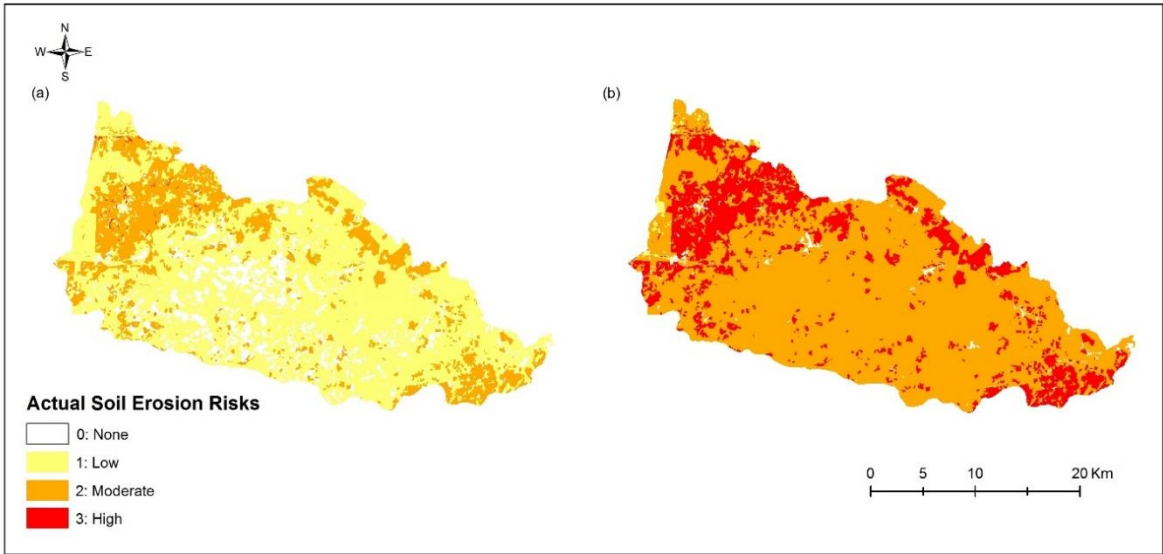374   calculator" tool. Figure 8 reveals the outcome under both scenarios.
375
376
377

378

379
380   **Figure 8.** Actual Soil Erosion risk map of the Claise under (a) current vegetation cover and (b) the alternative
381   pondless scenario.
382
383   The Actual Soil Erosion map was cross–checked against: Institut National de la Recherche
384   Agronomique (INRA) 2000 erosion maps and the combined GIS sol–INRA–SOeS 2011 maps [79].
385   These were produced following the Modèle d'évaluation spatiale de l'aléa d'érosion des sols
386   (MESALES). By this comparison, it is concluded that there is a good agreement between these maps
387   (Table 6). In addition, since INRA maps are not completely adequate to be considered at the basin
388   scale [80], the established erosion maps are considered for the no–erosion zones, overcoming, this
389   way, the challenge of coarse representation.
390
391   **Table 6.** Verification of the established erosion map.

Classes	Low	Moderate	High	Validation points
Low	76	10	0	86
Moderate	15	14	8	37
High	0	0	11	11
Total	91	24	19	134

392
393   The overall accuracy was determined to be 75%, while the computed Cohen's Kappa coefficient
394   was found to be 0.7; this indicates a substantial agreement between the two models.
395   From Figure 8, three main results can be drawn:
396   (1) The role of vegetation cover in changing erosion risks is solidified. This is particularly
397   reflected by the setting of the Claise basin due to the agricultural and grass cover. By comparing the
398   Actual Soil Erosion risk map with the Potential Soil Erosion risk map and statistics, a shift of erosion
399   risk classes is observed. As mentioned in Section 4.1.4, considering the potential soil erosion risks,
400   and ignoring the vegetation cover, low, moderate and high–risk areas take over 3%, 96.5% and 0.5%
401   of the total basin area, accordingly. When the vegetation cover layer was taken into account the
402   resulting Actual Soil Erosion risk shifted to 65.66%, 21.68% and 0.18%, for low, moderate and high–
403   risk areas. These observations solidify that vegetative cover is the most influential aspect for erosion
404   assessment. In further detail regarding the vegetation cover layer, areas corresponding to agricultural
405   classes are seen to have higher erosion risks than areas with different land cover types. This is in
406   agreement with Verheijen et al. (2009) [81] observations that despite the considerable effect of soil
407   type, topography and climatic conditions, the major influencer of soil erosion is the vegetative cover,
408   especially cultivated areas.

409 (2) The remainder 12.48% of the Actual Soil Erosion risk map is the no–erosion zone. As seen in
410 Figure 7(a), most of the no–erosion zone corresponds to the concentration area of ponds while the
411 remainder 1.48% represents the Claise River. The ponded area represents 88.23 km² of the Claise
412 under no risk of erosion making these ponds a counter–erosion zone.
413 (3) At a graphical scale, a complete shift from low to moderate risks is observed. Table 7 presents
414 the statistical difference between the Actual Soil Erosion risks with current vegetation cover and those
415 of the pondless scenario. From Table 7, the effective role of ponds as an erosion countermeasure is
416 revealed.
417
418 **Table 7.** Actual Soil Erosion risk (ASE) for the Claise basin under current and simulated vegetation cover

Erosion risks	ASE with current vegetation cover –Area (km²)	ASE with simulated vegetation cover (absence of ponds) – Area (km²)	ASE with current vegetation cover– percentage (%)	ASE with simulated vegetation cover (absence of ponds) – percentage (%)
None	88.23	7.92	12.48	1.12
Low	464.21	3.6	65.66	0.52
Moderate	153.27	543	21.68	76.8
High	1.272	152.4	0.18	21.56

419
420 Additionally, the impact of ponds on erosion at the scale of the basin is revealed. Not only did
421 the no–erosion and low–erosion classes decrease by 11.36% and 65.14%, in the absence of ponds
422 scenario, but also the moderate and high–erosion risks increased by 55.12% and 21.38%, respectively.
423 These changes are due to several reasons:
424 (1) The most evident reason is that ponds effectively and directly nullify splash erosion in the
425 areas they occupy.
426 (2) Their widespread, yet dense, positioning throughout the basin, counteracts runoff erosion in
427 a twofold way: first, by intercepting sediment transport by overland flow retaining, this way,
428 sediments and preventing them to reach the streams, and second, by slowing surface runoff and thus,
429 abating its erosive force. Despite the fact that the low–slope topography does not particularly favor
430 runoff erosion, let alone high velocities of overland flow, this obviously has some effect, especially in
431 cases of intense rainfall events.
432 (3) Their dense aggregation in the basin attributes them the role of cascade run–of–the–river
433 dams, containing sediments.
434 (4) Their large density and chain sequence where the retention effect is greatly amplified (factor
435 of 2179 ponds) [38].
436 (5) The highly erodible setting of the basin resulting from a challenging pedology.

437 *3.2. Sediment transport in a limnologically rich setting*

438 Sediment transport in the Claise was simulated using the SWAT model. The model was
439 calibrated using the SUFI–2 algorithm of SWATCUP following Jalowska and Yuan (2019) [38]
440 proposed sequential calibration for settings characterized by the presence of water impoundments.
441 As mentioned previously, due to the unavailability of sediment measurements for this study, only a
442 hydrologic calibration was performed with the most related sensitive parameters (Table 8). Results
443 of the hydrologic calibration yielded an R^2 of 0.7 during calibration and 0.67 during validation.
444
445
446

447   **Table 8.** Sensitivity analysis for calibration of the SWAT model

Parameter Name	t–Stat	P–Value	Fitted value
R__WET_NVOL.pnd	−37.52	0.00	0.823
V__GW_DELAY.gw	−31.39	0.00	52.325
R__PND_SED.pnd	1.62	0.11	318.100
V__GWQMN.gw	1.59	0.11	1.461
R__SPCON.bsn	−1.35	0.18	0.005
R__CN2.mgt	1.29	0.20	0.564
R__PND_NSED.pnd	1.23	0.22	2420.81
R__USLE_K.sol	−0.97	0.33	0.209
V__ALPHA_BF.gw	−0.90	0.37	0.529
R__NDTARG.pnd	0.44	0.66	49.890
R__PND_FR.pnd	0.15	0.88	0.644
R__USLE_P.mgt	−0.11	0.91	0.188
R__IGRO.mgt	−0.04	0.97	0.080

448
449   As a result of an exhaustive hydrologic calibration, the average sediment yield of the Claise
450   basin for the studied period under current and alternative conditions is presented in Figure 9.
451
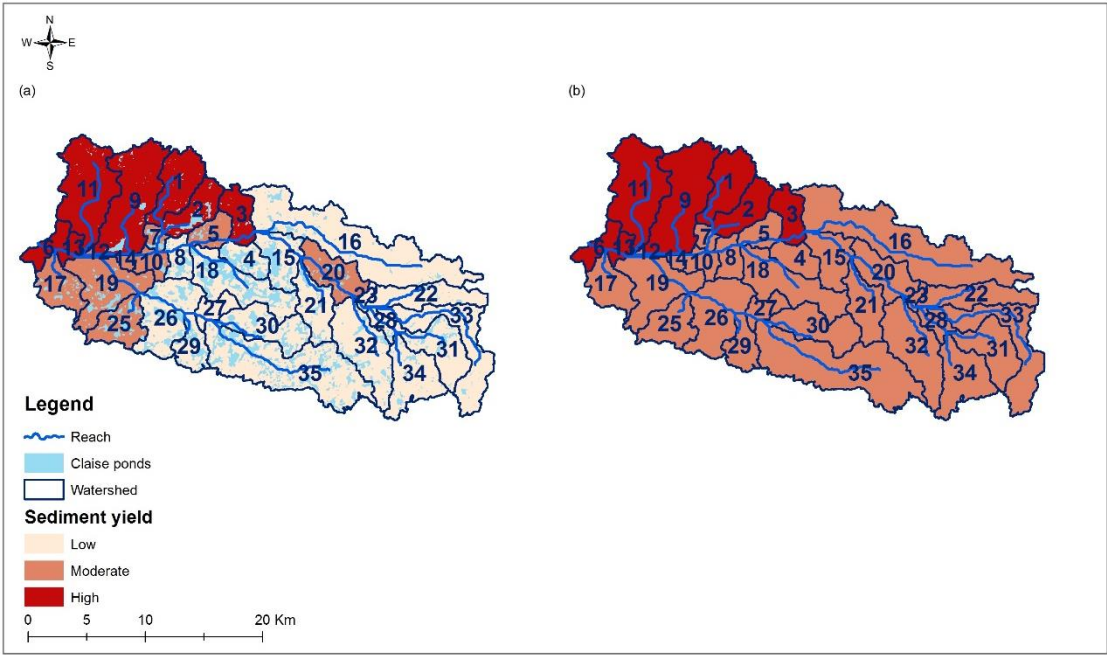
452
453   **Figure 9.** Sediment yields of the Claise basin under (a) current conditions and (b) the pondless scenario

454   As can be seen from Figure 9, low sediment yields correspond to ponded sub–basins in contrast
455   to pondless sub–basins which present lower soil loss rates. However, this gradient varies according
456   to the setting of the ponds in these sub–basins. Despite that sub–basins 1 and 9 contain a small
457   number of ponds, these correspond to areas of high sediment yield as a result of their dominant
458   agricultural cover and their location in the basin's steepest areas. This shows that the presence of
459   ponds alone is not sufficient to alter the sediment yields. In fact, the setting of ponds under the form
460   of a collective dense network is the main modifier of sediment transport patterns. In order to further
461   highlight the impact of ponds, alternative scenario testing was performed where a pondless land
462   occupation setting was re–input to the calibrated SWAT model in order to determine subsequent
463   sediment transport changes. Results of sediment yields, highlighting the impact of ponds, are
464   presented in Table 9.
465

466　　　　　　　　　　　**Table 9.** Shifts of sediment yields as a result of pond presence or absence

Sediment yield	Pond presence (Area km²; Percentage %)	Pond absence (Area km²; Percentage %)
Low	365.07 ; 63.31	0 ; 0
Moderate	89.23 ; 15.47	454.30 ; 78.79
High	122.27 ; 21.20	122.27 ; 21.20

467
468　　　　In the low sediment yield sub–basins, where the vast majority of ponds lies, occupying a large
469　portion of the sub–basins they are located in, the land cover change from pond to grasslands is far
470　too great and the effect of ponds presence/absence is quite obvious.

471　**4. Conclusions**

472　　　　An investigation of the pond–induced effects on soil erosion and sediment transport of
473　limnologically rich basins was presented. Through this task, recommendations of the European
474　framework for the Thematic Strategy on Soil Protection were addressed by revealing the different
475　levels of soil loss, represented by providing an insight to the investigation of erosion–prone regions
476　and sediment yield zones of different levels. Furthermore, recommendations of the DCE regarding
477　the behavioral understanding of hydromorphological alternating factors (ponds as hydro–
478　sedimentary elements), at the basin scale, were also considered. Despite the Claises' weakly
479　structured pedology, resulting in high erodibility, the Claise was found to have low erosion risks and
480　sediment transport rates due to several reasons, like the evenly distributed rainfall, the relatively flat
481　topography, and most importantly due to the presence of its dense pond network that acts as a
482　natural measure against soil erosion. This was solidified by simulating a scenario where ponds were
483　substituted by grasslands. After replacing ponds by a protective vegetative cover, all erosion risks
484　and sediment yield classes of the Claise significantly varied: no and low-erosion risk zones decreased,
485　while moderate and high-erosion risk zones increased. Regarding sediment transport, the
486　replacement of ponds by grasslands led to a complete disappearance of low sediment yield zones
487　and considerable increases of moderate and high sediment yield zones. Accordingly, the "safe" soil
488　loss status of the Claise can be attributed to the low soil loss rates of the Claise basin to the presence
489　of these ponds. Despite their protection against soil erosion, however, their presence in very large
490　numbers might cause a distortion in the sediment balance of the underlying rivers. Such cases may
491　lead to sediment starvation and force the river to engage in increasing streambed and bank erosion
492　[82]. Therefore, the use of the presented approach may serve as an efficient tool towards the
493　orientation of future decisions regarding the proliferation or cease of ponds depending on their effect.

494　**Author Contributions:** Conceptualization, Rachid Nedjai and Mario Al Sayah.; Data curation, Mario Al Sayah.;
495　Methodology, Mario Al Sayah and Rachid Nedjai.; Project administration, Rachid Nedjai, Chadi Abdallah, and
496　Michel Khouri.; Supervision, Rachid Nedjai, Konstantinos Kaffas, Chadi Abdallah and Michel Khouri;
497　Validation, Mario Al Sayah.; Visualization, Mario Al Sayah, Konstantinos Kaffas.; Writing—original draft, Mario
498　Al Sayah, Konstantinos Kaffas., Writing——review and editing, Mario Al Sayah, Konstantinos Kaffas ,Rachid
499　Nedjai, , Chadi Abdallah, Michel Khouri.

505　**Conflicts of Interest:** The authors declare no conflict of interest.

506　**References**

507   1.   Gyamfi C.; Ndambuki J.M.; Salim R.W. Simulation of sediment yield in a semi–arid river basin under
508   changing land use: An integrated approach of hydrologic modelling and principal component analysis.
509   *Sustainability* **2016**; *8(1133)*, 1–17. DOI: 10.3390/su8111133

510   2.   Dwarakish G.S.; Ganasri B.P. Impact of land use change on hydrological systems: A review of current
511   modeling approaches. *Cogent Geosci* **2015**; *1*, 1–18. DOI: 10.1080/23312041.2015.1115691

512   3.   van Rijn L.C. *Principles of Sediment Transport in rivers, estuaries and coastal seas*. Aqua Publications:
513   Amsterdam, Netherlands, 1993; p. 690.

514   4.   Esa E.; Assen M.; Legass A. Implications of land use/cover dynamics on soil erosion potential of agricultural
515   watershed, northwestern highlands of Ethiopia. *Env Syst Res* **2018**; *7(21)*, 1–14. DOI:
516   https://doi.org/10.1186/s40068-018-0122-0

517   5.   Aksoy H.; Mahe G.; Meddi M. Modeling and Practice of Erosion and Sediment Transport under Change.
518   *Water* **2019**; *11(1665)*, 1–9. DOI: 10.3390/w11081665

519   6.   Zhang S.; Li Z.; Lin X.; Zhang C. Assessment of Climate Change and Associated Vegetation Cover Change
520   on Watershed–Scale Runoff and Sediment Yield. *Water* **2019**; *11(7)*, 1–20. DOI: 10.3390/w11071373

521   7.   Bussi G.; Dadson S.J.; Prudhomme C.; Whitehead P.G. Modelling the future impacts of climate and land–
522   use change on suspended sediment transport in the River Thames (UK). *J. Hydrol* **2016**; *542*, 357–72. DOI:
523   https://doi.org/10.1016/j.jhydrol.2016.09.010

524   8.   Ffolliott P.F.; Brooks K.C.; Neary D.G.; Tapia P.R.; Chevesich P.G. *Soil Erosion and Sediment Production on
525   Watershed Landscapes: Processes and Control*. UNESCO Special Technical Publication No. 32, Montevideo,
526   Uruguay, 2013; p. 73.

527   9.   Aga A.O.; Chane B.; Melesse A.M. Soil erosion modelling and risk assessment in data Scarce Rift Valley
528   Lake Regions, Ethiopia. *Water (Switzerland)* **2018**; *10(1684)*, 1–17. DOI: 10.3390/w10111684

529   10.   Laflen J.M.; Lane L.J.; Foster G.R. WEPP: A new generation of erosion prediction technology. *J Soil Water
530   Conserv* **1991**; *46(1)*, 34–38.

531   11.   Flanagan D.C.; Gilley J.E.; Franti T.G. Water Erosion Prediction Project (WEPP) Development History,
532   Model Capabilities and Future Enhancements. *Am. Soc. Agric. Biol Eng.* **2007**; *50(5)*, 1603–1612.

533   12.   Wischmeier, W.H.; Smith D.D. *Predicting rainfall erosion losses from cropland east of the Rocky Mountains–guide
534   for selection of practices for soil and water conservation*. Agriculture Handbook No. 282, USDA, Washington,
535   USA, 1965.

536   13.   Williams J.R. Sediment–Yield Prediction with Universal Soil Loss Equation Using Runoff Energy Factor. In
537   Present and Prospective Technology for Predicting Sediment Yields and Sources. Proceedings of the
538   Sediment Yield Workshop, Oxford, 1975; p. 244–252.

539   14.   Renard K.G.; Foster G.R.; Weesies G.A.; McCool D.K.; Yoder D.C. Predicting soil erosion by water: a guide
540   to conservation planning with the Revised Universal Soil Loss Equation (RUSLE) (Vol. 703). Washington
541   DC; 1997.

542   15.   Renard K.G.; Yoder D.C.; Lightle D.T.; Dabney S.M. *Universal Soil Loss Equation and Revised Universal Soil
543   Loss Equation.* In: Morgan RPC, Nearing M., editors. *Handbook of Erosion Modelling*. Blackwell Publishing,
544   2011; p. 137–66.

545   16.   Arnold J.G.; Srinivasan R.; Muttiah R.S.; Williams J.R. Large area hydrologic modeling and assessment part
546   I: Model development. *J. Am. Water. Resour. Assoc.* **1998**; *34(1)*, 73–89. DOI: https://doi.org/10.1111/j.1752-
547   1688.1998.tb05961.x

548   17.   Samaras A.G.; Koutitas C.G. Modeling the impact of climate change on sediment transport and
549   morphology in coupled watershed–coast systems : A case study using an integrated approach. *Int. J.
550   Sediment. Res.* **2015**; *29(3)*. 304–315. DOI: http://dx.doi.org/10.1016/S1001–6279(14)60046–9

551   18.   Kaffas K.; Hrissanthou V.; Sevastas S. Modeling hydromorphological processes in a mountainous basin
552   using a composite mathematical model and ArcSWAT. *Catena* **2018**; *162(April 2017)*, 108–129.

553   19.   Kaffas K.; Righetti M.; Avesani D.; Spiliotis M.; Hrissanthou V. Coupling CFSv2 with ArcSWAT for
554   seasonal hydrological forecasting in a Mediterranean basin. 11th World Congress on Water Resources and
555   Environment (EWRA 2019). Madrid, Spain; 2019. pp. 459–60.

556   20.   Napoli M.; Massetti L.; Orlandini S. Hydrological response to land use and climate changes in a rural hilly
557   basin in Italy. *Catena* **2017**; *157(October 2016)*, 1–11. DOI: http://dx.doi.org/10.1016/j.catena.2017.05.002

558   21.   Alemaw D.; Ayana E.K.; Legesse E.S.; Moges M.M.; Tilahun S.A.; Moges M.A. Estimating reservoir
559   sedimentation using bathymetric differencing and hydrologic modeling in data scarce Koga watershed,
560   Upper Blue Nile, Ethiopia. *J. Agric. Environ. Int. Dev.* **2016**; *110(2)*, 413–27. DOI: 10.12895/jaeid.20162.519

561 22. Dhami B.S.; Pandey A. Comparative Review of Recently Developed Hydrologic Models. J. *Indian. Water.*
562   *Resour Soc.* **2013**; *33(3)*, 34–42.
563 23. Abbaspour K.C; Vaghefi S.A.; Srinivasan R. A guideline for successful calibration and uncertainty analysis
564   for soil and water assessment: A review of papers from the 2016 international SWAT conference. *Water*
565   *(Switzerland)* **2017**; *10(6)*, 1–18. DOI: https://doi.org/10.3390/w10010006
566 24. Biggs J.; von Fumetti S.; Kelly–Quinn M. The importance of small waterbodies for biodiversity and
567   ecosystem services: implications for policy makers. *Hydrobiologia* **2016**; *793(1)*, 3–39. DOI: 10.1007/s10750-
568   016-3007-0
569 25. Mujere N.; Eslamian S. *Climate Change Impacts on Hydrology and Water Resources*. In: Eslamian S, editor.
570   *Handbook of Engineering Hydrology Modeling, Climate Change and Variability*. CRC–Press, 2014; p. 114–125.
571 26. Downing J.A.; Prairie Y.T.; Cole J.J.; Duarte C.M.; Tranvik L.J.; Striegl R.G.; et al. The global abundance and
572   size distribution of lakes, ponds, and impoundments. *Limnol. Ocean.* **2006**; *51(5)*, 2388–2397. DOI:
573   https://doi.org/10.4319/lo.2006.51.5.2388
574 27. Miracle M.R.; Oertli B.; Céréghino R.; Hull A. Preface: conservation of european ponds–current knowledge
575   and future needs. *Limnetica* **2010**; *29(1)*,1–8. ISSN: 0213-8409
576 28. Céréghino R.; Biggs J.; Oertli B.; Declerck S. The ecology of European ponds: defining the characteristics of
577   a neglected freshwater habitat. *Hydrobiologia* **2008**; *597*, 1–6. DOI: https://doi.org/10.1007/s10750-007-9225-8
578 29. Williams P.; Whitfield M.; Biggs J. How can we make new ponds biodiverse? A case study monitored over
579   7 years. *Hydrobiologia* **2008**; *597*, 137–48. DOI: https://doi.org/10.1007/978-90-481-9088-1_12
580 30. Céréghino R.; Boix D.; Cauchie H.M.; Martens K.; Oertli B. The ecological role of ponds in a changing world.
581   *Hydrobiologia* **2014**; 723(1),1–6. DOI: https://doi.org/10.1007/s10750-013-1719-y
582 31. Sharpley A.N.; Bergström L.; Aronsson H.; Bechmann M.; Bolster C.H.; Börling K.; et al. Future agriculture
583   with minimized phosphorus losses to waters: Research needs and direction. *Ambio* **2015**; *44(2)*, 163–179.
584   DOI: https://doi.org/10.1007/s13280-014-0612-x
585 32. Oertli B.; Frossard P.A. Mares et étangs: Ecologie, conservation, gestion, valorisation. 1st ed. Presses
586   polytechniques et universitaires romandes; 2013. 512 p.
587 33. Hill M.J.; Hassall C.; Oertli B.; Fahrig L.; Robson B.J.; Biggs J.; et al. New policy directions for global pond
588   conservation. *Conserv Lett* **2018**; *11*, 8. DOI: https://doi.org/10.1111/conl.12447
589 34. Indermuehle N.; Oertli B.; Biggs J.; Céréghino R.; Grillas P.; Hull A.; et al. Pond conservation in Europe: the
590   European Pond Conservation Network (EPCN). Int. Vereinigung. Für. Theor. Und. Angew. Limnol.
591   Verhandlungen. **2008**; *30(3)*, 446–448. DOI: https://doi.org/10.1080/03680770.2008.11902163
592 35. Mujere N.; Eslamian S. *Impact of Urbanization on Runoff Regime*. In: Eslamian S, editor. *Handbook of*
593   *Engineering Hydrology Modeling, Climate Change and Variability*. CRC–Press, 2014; p. 114–125.
594 36. Nedjai R. ; Azaroual A. ; Chlif K. ; Bensaid A. ; Al Sayah M. ; Ysbaa L. Impact of Ponds on Local Climate:
595   A Remote Sensing and GIS Contribution Application to the Ponds of Brenne (France). *J. Earth. Sci. Clim.*
596   *Change.* **2018**; *9(12)*: 10.
597 37. Benarrous R. La Grande Brenne aux périodes préindustrielles (Indre) Contribution à l'histoire des
598   paysages, des étangs et des relations sociétés / milieux dans une zone humide continentale. Approches
599   historique, archéologique et paléo–environnementale. Université de Paris I – Panthéon Sorbonne; 2009.
600 38. Jalowska A.M.; Yuan Y. Evaluation of SWAT Impoundment Modeling Methods in Water and Sediment
601   Simulations. *J. Am. Water. Resour. Assoc.* **2019**; *55(1)*, 209–27. DOI: https://doi.org/10.1111/1752-1688.12715
602 39. Clifford C.C.; Heffernan J.B. Artificial Aquatic Ecosystems. *Water* **2018**; *10(1096)*,1–30. DOI:
603   https://doi.org/10.3390/w10081096
604 40. Ebel J.D.; Lowe W.H. Constructed Ponds and Small Stream Habitats: Hypothesized Interactions and
605   Methods to Minimize Impacts. *J. Water. Resour. Prot.* **2013**; *05(07)*, 723–31.
606 41. Ismail T.; Othman M.A.; Fadzil A.B.; Zainuddin Z.M. Deposition of Sediments in Detention Pond.
607   *Malaysian. J. Civ. Eng.* **2010**; *22(1)*, 95–118.
608 42. Declerck S.; De Bie T.; Ercken D.; Hampel H.; Schrijvers S.; van Wichelen J.; et al. Ecological characteristics
609   of small farmland ponds: Associations with land use practices at multiple spatial scales. *Biol. Conserv.* **2006**
610   , 523–532.
611 43. Winfield Fairchild G.; Velinsky D.J. Effects of Small Ponds on Stream Water Chemistry. *Lake. Reserv. Manag.*
612   **2006**; *22(4)*, 321–330.
613 44. Commission Européenne. La Directive–cadre européenne sur l'eau. 2000.

45. Biggs J.; Williams P.; Whitfield P.; Nicolet P.; Weatherby A. 15 years of pond assessment in Britain: results and lessons learned from the work of Pond Conservation. *Aquat. Conserv. Mar. Freshw. Ecosyst.* **2005**; *15*, 693–714.

46. Jeffries M. Local–scale turnover of pond insects: intrapond habitat quality and inter–pond geometry are both important. *Hydrobiologia* **2005**; *543*, 207–220.

47. Neitsch S.L.; Arnold J.G.; Kiniry J.R.; Williams J.R. Soil & Water Assessment Tool Theoretical Documentation Version 2009. Texas; 2011.

48. Guichané R. L'aménagement hydraulique de la Claise tourangelle et de ses affluents du Moyen–Âge à nos jours / Mills on the claise and its tributaries in Indre–et–Loire from the Middle Ages to modern times. Rev Archeol Centre France. **1993**; *32*, 109–152.

49. SANDRE. Fiche cours d'eau la Claise (L6—0200). 2012.

50. Joly D.; Brossard T.; Cardot H.; Cavailhes J.; Hilal M.; Wavresky P. Les types de climats en France, une construction spatiale – Types of climates on continental France, a spatial construction. *Cybergéo Eur J Geogr* . **2010**; *501*, 1–23.

51. Fischer G.; Nachtergaele F.; Prieler S.; van Velthuizen H.T.; Verelst L.; Wiberg D. Global Agro–ecological Zones Assessment for Agriculture (GAEZ 2008). Rome, Italy; 2008.

52. Dauphin P. ; Mansons J. ; Pellé B. ; Airault V. ; Trotignon J. ; Boyer P. ; et al. Document d'objectifs des sites Natura 2000 FR2410003 "Brenne" et FR2400534 "Grande Brenne." 2012.

53. Bouscasse H. ; Defrance P. ; Amand B. ; Grandmougi B. ; Strosser P. ; Beley Y. Amélioration des connaissances sur les fonctions et usages des zones humides : évaluation économique sur des sites tests le cas des étangs de la Grande Brenne. AcTeon et ecoVita, 2011.

54. Arnold J.G.; Moriasi D.N. ; Gassman P.W. ; Abbaspour K.C. ; White M.J. ; Sirnivasan R. ; et al. SWAT: Model use, Calibration, and Validation. *Am. Soc. Agric. Biol. Eng.* **2012**; *55(4)*, 1491–1508.

55. Gassman P.W.; Reyes M.R.; Green C.H.; Arnold J.G. The Soil and Water Assessment Tool: Historical Development, Applications, and Future Research Directions. *Am. Soc. Agric. Biol. Eng.* **2007**; *50(4)*, 1211–1250.

56. Epelde A.M; Cerro I.; Sánchez–Pérez J.M.; Sauvage S.; Srinivasan R.; Antigüedad I. Application of the SWAT model to assess the impact of changes in agricultural management practices on water quality. *Hydrol. Sci. J.* **2014**; *60(5)*, 825–843.

57. Srinivasan R.; Zhang X.; Arnold J. SWAT ungauged: Hydrological budget and crop yield predictions in the Upper Mississippi river basin. *Trans ASABE.* **2010**; *53(5)*, 1533–1546.

58. Neitsch S.L.; Arnold J.G.; Kiniry J.R.; Rinivasan R.S.; Williams J.R. Soil and Water Assessment Tool User's Manual – Version 2000. Texas; 2002.

59. Arnold J.G.; Kiniry J.R.; Srinivasan R.; Williams J.R.; Haney E.B.; Neitsch S.L. Soil & Water Assessment Tool Input/Output Documentation Version 2012. Texas; 2012, p. 541

60. Kaffas K.; Hrissanthou V. Annual sediment yield prediction by means of three soil erosion models at the basin scale. Proceedings of the 10th World Congress of EWRA "Panta Rhei", Athens, Greece, 5–9 July 2017; pp. 1346–1352.

61. CORINE, 1992. CORINE Soil erosion risk and important land resources - in the southern regions of the European Community, Europe ; pp. 541

62. Fournier F. Climat et Erosion: La relation entre l'Erosion du sol par l'Eau et les precipitations Atmospheriques. Presses Universitaires De France, editor. Paris: Publication de l'Institut d'études roumaines; 1960. 201 p.

63. Gaussen H. Bioclimatic Map of Mediterranean Zone. Paris; 1963.

64. Durand Y.; Brun E.; Mérindol L.; Guyomarc'h G.; Lesaffre B.; Martin E. A meteorological estimation of relevant parameters for snow models. *Ann. Glaciol.* **1993**;*18*, 65–71.

65. Moriasi D.N.; Arnold J.G.; van Liew M.W.; Bingner R.L.; Harmel R.D.; Veith T.L. Model Evaluation Guidelines for Systematic Quantification of Accuracy in Watershed Simulations. *Trans ASABE* **2007**; *50(3)*, 885–900.

66. Hallouz F.; Meddi M.; Mahé G.; Alirahmani S.; Keddar A. Modeling of discharge and sediment transport through the SWAT model in the basin of Harraza (Northwest of Algeria). *Water. Sci.* **2018**; *32*, 79–88.

67. Buakhao W.; Kangrang A. DEM Resolution Impact on the Estimation of the Physical Characteristics of Watersheds by Using SWAT. *Adv Civ Eng*. **2016**; 2016, 9.

667   68.   Polanco E.I.; Fleifle A.; Ludwig R.; Disse M. Improving SWAT model performance in the upper Blue Nile
668   Basin using meteorological data integration and subcatchment discretization. *Hydrol. Earth. Syst Sci.* **2017**;
669   *21(9)*, 4907–4926.
670   69.   USDA Soil Conservation Service. National engineering handbook, Section 4: Hydrology. NEH Notice 4–
671   102. Washington, DC.; 1972.
672   70.   Saxton K.; Rawls W.J. Soil Water Characteristic Estimates by Texture and Organic Matter for Hydrologic
673   Solutions. *Soil. Sci. Soc. Am. J.* **2006**; *70*, 1569–1578.
674   71.   Al Sayah M.J.; Abdallah C.; Khouri M.; Nedjai R.; Darwich T. Application of the LDN concept for
675   quantification of the impact of land use and land cover changes on Mediterranean watersheds – Al Awali
676   basin – Lebanon as a case study. *Catena* **2019**; *176(May)*, 264–278.
677   72.   Périé C.; Ouimet R. Organic carbon, organic matter and bulk density relationships in boreal forest soils.
678   Can *J. Soil. Sci.* **2008**; *88(3)*,315–325.
679   73.   Post D.F.; Fimbres A.; Matthias A.D.; Sano E.; Accioly L.; Batchily A.K.; et al. Predicting Soil Albedo from
680   Soil Color and Spectral Reflectance Data. *Soil. Sci. Soc. Am. J.* 2000; *64(May–June)*,1027–1034.
681   74.   Pearson K. Notes on regression and inheritance in the case of two parents. *Proc. R. Soc. London*. **1985**; *58*,
682   240–242.
683   75.   SWAT. SWAT Weather Data and Tools [Internet]. 2019 [cited 2019 Mar 8]. Available from:
684   https://swat.tamu.edu/software/
685   76.   Almendinger J.E.; Murphy M.S.; Ulrich J.S. Use of the Soil and Water Assessment Tool to Scale Sediment
686   Delivery from Field to Watershed in an Agricultural Landscape with Topographic Depressions. *J. Environ.*
687   *Qual.* **2014**; *43(1)*, 9–17.
688   77.   Wang X.; Yang W.;Melesse A.M. Using Hydrologic Equivalent Wetland Concept within SWAT to Estimate
689   Streamflow in Watersheds with Numerous Wetlands. *Trans. Am. Soc. Agric. Eng*. **2008**; *51(1)*, 55-72. DOI:
690   10.13031/2013.24227
691   78.   Ahmed S.I.; Rudra R.P.; Gharabaghi B.; Mackenzie K.; Dickinson W.T. Within–Storm Rainfall Distribution
692   Effect on Soil Erosion Rate. *ISRN Soil. Sci*. **2012**; *2012*,1–7.
693   79.   Akale A.T.; Dagnew D.C.; Belete M.A.; Tilahun S.A.; Mekruia W.; Steenhuis T.S. Impact of Soil Depth and
694   Topography on the Effectiveness of Conservation Practices on Discharge and Soil Loss in the Ethiopian
695   Highlands. *Land* **2017**;*6(78)*, 1–17.
696   80.   Gis Sol, Inra, SOeS. Aléa d'érosion des sols en 2000. Orléans; 2000.
697   81.   Verheijen F.G.A.; Jones R.J.A.; Rickson R.J.; Smith C.J. Tolerable versus actual soil erosion rates in Europe.
698   *Earth–Science. Rev.* **2009**; 94, 23–38.
699   82.   Kondolf G.M. Hungry water: Effects of dams and gravel mining on river channels. *Environ. Manage*. **1997**;
700   *21(4)*, 533–551.